

---

PHOTOCHEMISTRY

---

## On the Possibility of a priori Quantitative Prediction of the Quantum Yield of a Photochemical Reaction

V. I. Baranov, L. A. Gribov, I. V. Mikhailov, and N. I. Potesnaya

*Vernadsky Institute of Geochemistry and Analytical Chemistry, Russian Academy of Sciences,  
ul. Kosygina 19, Moscow, 119991 Russia*

*e-mail: l\_gribov@mail.ru*

Received September 8, 2014

**Abstract**—The possibility of performing predictive calculations of the kinetics and quantum yields of photochemical transformations of polyatomic molecules with satisfactory accuracy has been shown. Taking into account the physically grounded requirements imposed and rather stringent constraints on the prediction error (less than 50%), a satisfactory theoretical result has been obtained for all of the considered reactions of three chemically different types. In most cases (eight out of ten reactions), the deviation from the experimental data was less than 20%. Model parameters have high transferability in a series of similar reactions, thereby ensuring the predictive character of simulation of photochemical processes using the method developed earlier. In complicated cases, it is possible to a priori theoretically assess the type of the reaction of interest and its physicochemical characteristics.

DOI: 10.1134/S0018143915020022

Stimulation of chemical reactions by the energy of absorbed photons is very effective and offers great opportunities, in particular: treatment of a molecular object of any complexity, a wide variety of radiation (excitation) wavelengths, broad ranges of excitation-signal intensity and irradiation time (from femtoseconds to hours), controlling chemical reactions by varying the excitation signal during phototransformation, etc.

The computer simulation of such processes at the quantitative level (at least by order of magnitude) becomes of the greatest importance, inasmuch as it will make it possible to quite comprehensively predict the events, conduct target-oriented planning of experimental research, and design the “molecular machines.”

Qualitative theoretical photochemistry [1–17] fails to give a priori quantitative estimates (even at the order-of-magnitude level) of important characteristics, such as quantum yields of reactions. However, some progress made recently in theoretical photochemistry—development of both general quantum theory of molecular transformations [18, 19] and an approach to quantitative description of photochemical processes [20–25]—opens up new opportunities in this regard. The set of calculations of the kinetics and quantum yields of more than 15 reactions showed satisfactory agreement with experimental data at the quantitative level (prediction of orders of magnitude [20–24]).

In the approach that we develop, an empirical parameter is used that takes into account asymmetry

of the potential wells of molecular entities involved in phototransformation, the asymmetry consisting in significantly higher curvature of the energy surfaces at the edges of the wells than at the potential barrier. This is illustrated in Fig. 1, which schematically shows the potential energy surface corresponding to the two structural isomeric states of a molecular system and its cross section along the normal coordinates of these isomeric forms. Hereinafter, normalized normal coordinates  $X = Q/Q_0$  and  $X' = Q'/Q'_0$ , are used, where  $Q_0$  and  $Q'_0$  are the amplitudes of zero-point vibrations in the isomers. The idea is to use molecular models with extended potential surfaces, so that their shape will be correctly represented in the barrier region in which the overlap of the wave functions of the combining states of molecules is maximal and its value has a determining role in the probability of the nonradiative transition [18]. This region (and point  $X_B$  on the top of the barrier) is schematically shown in Fig. 1. It has been found [18] that the resulting distortion in the potential surface (and, hence, the wave functions) at the edges of the wells has a negligible effect on the magnitude of the overlap integral of the wave functions and, therefore, does not play a significant role in phototransformation. It is imperative that the introduced empirical parameter of the molecular model (“broadening parameter”) has the property of transferability in a series of related reactions (its optimal values vary within 50%) [20–24], and it is due to this property that calculations to predict the quantum yields and the kinetics of photochemical processes can be carried out in terms of this approach (molecular model). The

idea, its substantiation, and the substance of the model are detailed in [15, 20–25].

In [26] we proposed an improved approach consisting of using an optimized molecular model with allowance for the potential surface asymmetry differentiated in the normal coordinates. Unlike the previous model, the fitting (broadening) of potential functions is performed only in the normal coordinates for which the asymmetry (anharmonicity) due to the presence of a potential barrier is essential, not in all of the normal coordinates of the isomers combined in the structural transformation. This optimized model is more physically correct, and that is why it is of greater interest and needs detailed verification. As a criterion for the selection of these significant normal coordinates, a considerable displacement (greater than a certain “critical” value  $X_0$ ) of barrier vertex  $X_B$  (area of the greatest overlap of the wave functions of the combining states, see Fig. 1) relative to the position of the well minimum along these coordinates was taken. Analysis has shown that for the optimum value of  $X_0$  can be  $X_0 = 1/\sqrt{2}$ , corresponding to the point on the potential energy function at half the relevant zero-point oscillation energy. Thus, as shown by model calculations [26], the coordinates by which the potential function is fitted include only those affecting significantly the structural transformation of the molecules and exclude the coordinates uninvolved in the transformation. This selection makes it possible to reduce by two thirds the number of coordinates by which the potential surface and, accordingly, the wave functions are adjusted using the broadening parameter.

Calculations for six reactions of diene molecules, namely: (1) 2-methylbutadiene-1,3  $\rightarrow$  1-methylcyclobutene, (2) 2,3-dimethylbutadiene-1,3  $\rightarrow$  dimethylcyclobutene, (3) pentadiene-1,3  $\rightarrow$  3-methylcyclobutene, (4) 2,4-dimethylpentadiene-1,3  $\rightarrow$  trimethylcyclobutene, (5) 1-methoxybutadiene-1,3  $\rightarrow$  methoxycyclobutene, and (6) *cis*-butadiene-1,3  $\rightarrow$  cyclobutene showed [26] that this optimized model results in significantly better agreement with experimental data in comparison with the model used previously and the transferability of the parameter in the series of the reactions is enhanced; i.e., the optimized model for the series of diene molecules adequately reflects the molecular properties and is more efficient for the simulation of photochemical transformations.

To determine the effectiveness of the optimized model and its practicability as applied to predictive calculations of the kinetics and quantum yields of photochemical reactions of molecules, in this study we investigated the properties of the model parameters, namely, the “critical” quantity  $X_0$  and parameter  $u$ , which determines the magnitude of broadening for the potential surfaces. The study focused on their effect on the calculated value of the quantum yield and the transferability of their values in series of reactions of various types. To increase the representativeness and

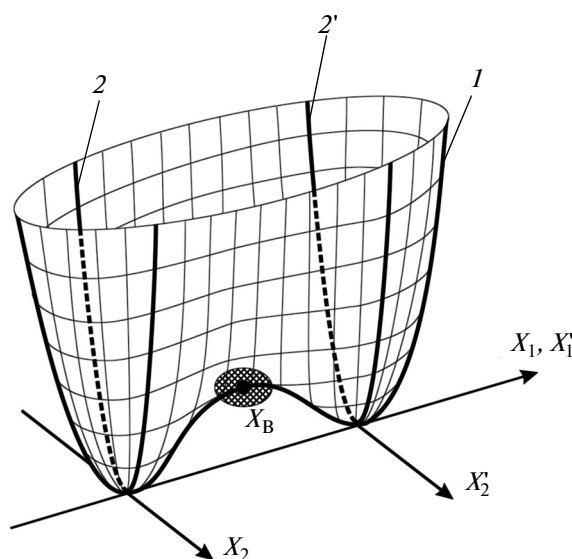
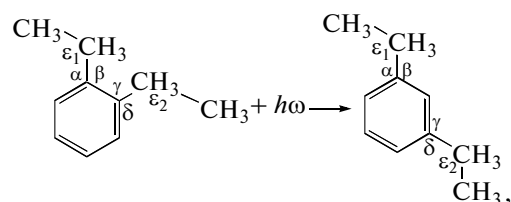


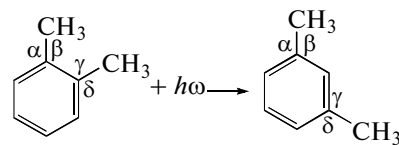
**Fig. 1.** Potential energy surface corresponding to two structural isomeric states of the molecular system, and the sections of the surface along normal coordinates (1)  $X_1(X'_1)$ , (2)  $X_2$  and (2')  $X'_2$ . The area of the greatest overlap of the wave functions of isomers (shaded) and barrier top point  $X_B$  are shown.

reliability of results, along with reactions (1)–(6) considered earlier [26], four reactions from other two series were additionally modeled, namely, dialkylaromatic molecules undergoing positional isomerization (reactions (7), (8)):

(7) *o*-diethylbenzene  $\rightarrow$  *m*-diethylbenzene

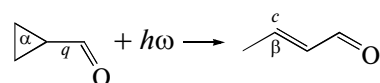


(8) *o*-xylene  $\rightarrow$  *m*-xylene



and aldehydes (ketones) undergoing ring opening in the cyclic (cyclopropyl) moiety (reactions (9), (10)):

(9) cyclopropylmethanal  $\rightarrow$  2-butenal



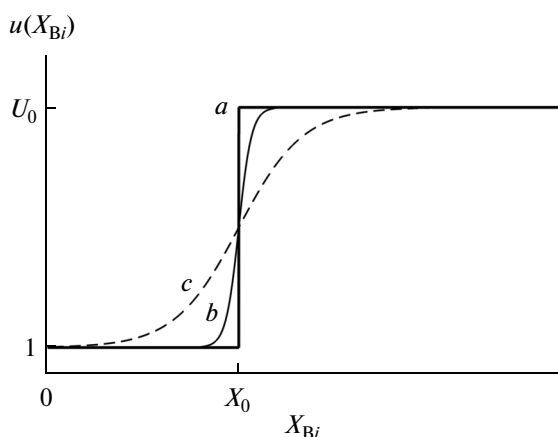
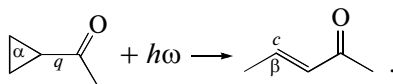


**Fig. 2.** Patterns of functional dependence of broadening parameter  $u(X_{Bi})$  used in the cases of (a) step function (1) and (b, c) smoothed step function (2) at different values of step smoothing parameter  $s$ : (b)  $s = 5$  or (c)  $s = 1$ .

**(10)** 3-cyclopropyletanal  $\rightarrow$  3-pentenone-2



The choice of these reactions is due to a number of their inherent features. These are the shift of a rather bulky substituent in the first group (reactions (7), (8)) and a relatively high quantum yield (an order of magnitude larger than in other reactions) and structural changes affecting directly the cyclic moiety in the second group (reactions (9), (10)).

The structural phototransformations of the molecules considered here are of three chemically different types: (I) reactions (1)–(6), (II) reactions (7) and (8), and (III) reactions (9) and (10). Combining them in a single study gives hope for greater generality of conclusions to be obtained than in the case of independent analysis of the reactions of each type.

We restrict our consideration in this case to structural isomerization reactions not only because of their relative simplicity, but also because structural changes play a key (determining) role in chemical transformation processes. Indeed, as shown previously [18], the decomposition reaction can be represented as a process of isomeric transition of the molecule in a metastable form that can easily and quickly fall apart because of its low stability. Synthesis reactions can be treated in the same manner [18].

## MOLECULAR MODEL

The main objective of simulation of photochemical reactions (and other structural transformations of molecules) is to obtain correct values of the overlap integrals of the wave functions for the resonant vibronic states of structural isomers involved in the

transformation. Consequently, it is necessary to describe in the best possible way the behavior of the wave functions in the potential barrier region (area of the greatest overlap as shown in Fig. 1). This area is characterized by point  $X_B$  of the top of the potential barrier having coordinates  $X_{Bi}(X'_{Bi})$  in the space of normalized normal coordinates.

For this purpose, as mentioned above, the formulation of the molecular model includes broadening of the vibrational wave functions, with the broadening magnitude being characterized by parameter  $u$ . In our optimized model, the asymmetry of potential energy surfaces was taken into account differentially in normal coordinates, so that broadening parameter  $u$  would be maximal for the coordinates by which the molecules undergo the most profound structural rearrangement. The broadening parameter in this case is functional in character,  $u(X_{Bi})$ , where  $X_{Bi}(X'_{Bi})$  are the coordinates (in the space of normalized normal coordinates) of point  $X_B$  describing the magnitude of structural changes during the reaction. Take that function  $u(X_{Bi})$  satisfies the following “boundary” conditions in terms of barrier coordinates:  $u(X_{\max}) = U_0$  and  $u(0) = 1$ , where  $X_{\max} = \max(X_{Bi})$  is the maximum value of coordinates  $X_{Bi}$  of point  $X_B$ , i.e., varies from 1 (no broadening, the displacement of the minima of potential energy surfaces of the isomers is zero for these coordinates) to a certain empirical value  $U_0$  (for coordinates by which the displacement of  $X_{Bi}$  is the greatest). Among the large set of types of functions that have been tested—linear, power-law, exponential, stepped, sigmoidal, etc. functions—the last two (step, sigmoidal) are of practical interest.

A step function has only two parameters, namely, upper bound  $U_0$  and discontinuity point  $X_0$  (“critical” value of coordinate  $X_{Bi}$ ):

$$u(X_{Bi}) = \begin{cases} U_0, & X_{Bi} > X_0 \\ 1, & X_{Bi} \leq X_0 \end{cases} \quad (1)$$

A smoothed step function (rational sigmoid function, arc tangent, hyperbolic tangent, error function, etc.) has three parameters: upper asymptote  $U_0$  and inflection point (point of maximum growth)  $X_0$  are complemented by parameter  $s$ , which determines the degree of step smoothing. For example, if the function has the form of hyperbolic tangent, we have:

$$u(X_{Bi}) = \frac{U_0 - 1}{2} \operatorname{th}[s(X_{Bi} - X_0)] + \frac{U_0 + 1}{2} \quad (2)$$

The plots of the functions are shown in Fig. 2. The most important factors determining the choice of the type of function  $u(X_{Bi})$  are as follows.

On one hand, a significant decrease in the number of normal coordinates for which the potential energy surface is refined with allowance for its asymmetry must be ensured, a development that corresponds to

the well-known fact of a small number of coordinates involved in a structural transformation process [18]. The smallness of the number of such coordinates is clearly seen from Fig. 3 showing typical histograms of their distribution by the values of  $X_{Bi}$ . The total number of coordinates of the combining isomeric structures that have the highest values of  $X_{Bi}$  and, hence, determine the structural transformation is generally two to four (especially for large polyatomic molecules); i.e., on the order of  $N_Q \approx 20\%$  of their total number or less. Experience in simulation of chemical reactions has shown that  $N_Q$  can be certainly assumed to be  $<50\%$ . In the following analysis, we will proceed from the requirement that  $N_Q \leq 45\%$ .

On the other hand, the broadening of the model surface should not lead to a change in the position of the area of the largest overlap of the functions, i.e., should not displace point  $X_B$  in the normal coordinate space, thereby ensuring unambiguity of the procedure for determining the resonant states in the simulation of structural transformation processes. The magnitude of the displacement is characterized by the angle of rotation  $\xi$  of the vector directed from the minimum of the potential well to point  $X_B$  in the top of the barrier, and this value, as has been shown in a large number of model calculations, should not exceed  $\xi = 0.4$  rad in order to meet the aforementioned requirement. This value will be used as the upper bound for  $\xi$  ( $\xi \leq 0.4$ ).

Smoothed step functions do satisfy these requirements unless parameter  $s$  has a very large value. The model calculations showed that for values of  $s$  acceptable in terms of these requirements ( $s \geq 5$ ; curve  $b$  in Fig. 2), the results negligibly differ from those obtained using  $u(X_i)$  represented as step function (1) (curve  $a$  in Fig. 2). For example, the quantum yields calculated with the use of the step function and the smoothed function with  $s \geq 5$  differ by less than 5%. Therefore, step function (1) is the most appropriate for describing the form of  $u(X_{Bi})$ . The parameters of this function and, hence, of the model used in the calculation procedure are  $U_0$  and  $X_0$ .

### CALCULATION OF QUANTUM YIELDS OF REACTIONS

The quantum yields of reactions (1)–(10) were calculated in terms of the molecular model described above.

To reveal the dependence of the quantum yields of the reactions on the values of model parameters  $U_0$ ,  $X_0$  and determine the optimal values of these parameters for groups of reactions of the same type, model calculations were performed in a wide range of values of the parameters. The calculations showed that the relationships of interest are similar in nature. As typical examples, their three-dimensional plots for reactions (1) and (5) are shown in Fig. 4. A characteristic feature of

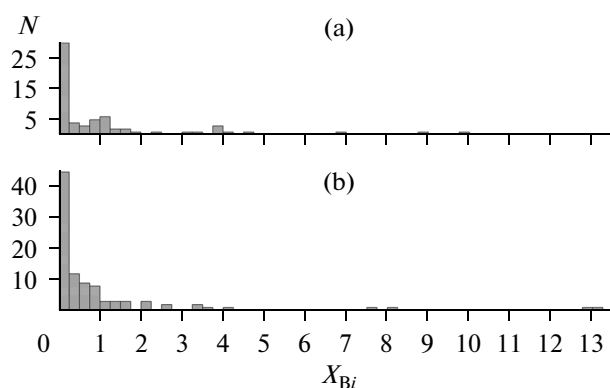


**Fig. 3.** Histograms of the distribution of normal coordinates over the values of barrier top coordinate  $X_{Bi}$  for reactions (a) (1) and (b) (4).  $N$  is the total number of coordinates of the combining isomers in the reaction, whose values of  $X_{Bi}$  lie in the preset range.

all of these reactions is a quite narrow band of  $U_0$  or  $X_0$  values in which the quantum yield varies from the minimum ( $\varphi_{\min} = 0$ ) to the maximum ( $\varphi_{\max}$ ) value allowable within the frame of this model. It is these bands that are of the greatest interest. It is very important that the experimental values of the quantum yield ( $\varphi_{\exp}$ ) for all of the above reactions lie in this range or in the immediate vicinity of it (reactions (9) and (10); deviation of no more than  $0.5\varphi_{\exp}$ , i.e., within 50% error). Consequently, this model makes it possible to select such values of  $U_0$  and  $X_0$  that will ensure the desired prediction at the level of at least their order of magnitude (see below for detail) and it is a very valuable result.

What is surprising at first glance is the appearance of the narrow “dips” (down to  $\varphi_{\text{calc}} = 0$ ) on the three-dimensional surfaces in the range of the parameters at which the quantum yields are close to  $\varphi_{\max}$ . However, the values of model parameters  $U_0$  and  $X_0$  associated with these dips are of no practical interest, since they correspond to such large values of broadening parameter  $U_0$  that the wave functions of the isomers overlap almost completely, not by the “tails” as it is typical of reactions [18]. Because of the oscillatory nature of the vibrational wave functions, their overlap of this type can lead to a nearly zero overlap integral and, consequently,  $\varphi_{\text{calc}} \approx 0$ , which is indeed the case observed for the given processes. Note that such an overlap of the functions corresponds to vibronic levels lying well above the potential barrier on energy scale and being already common for the combining isomeric forms. This situation corresponds to either superexcited states or structural rearrangements with a very low barrier and requires special theoretical analysis and special modeling approaches, which are beyond the scope of this paper.

Thus, the calculations showed that within the framework of this model, it is possible to choose such a set of  $U_0$  and  $X_0$  values at which agreement of calcu-

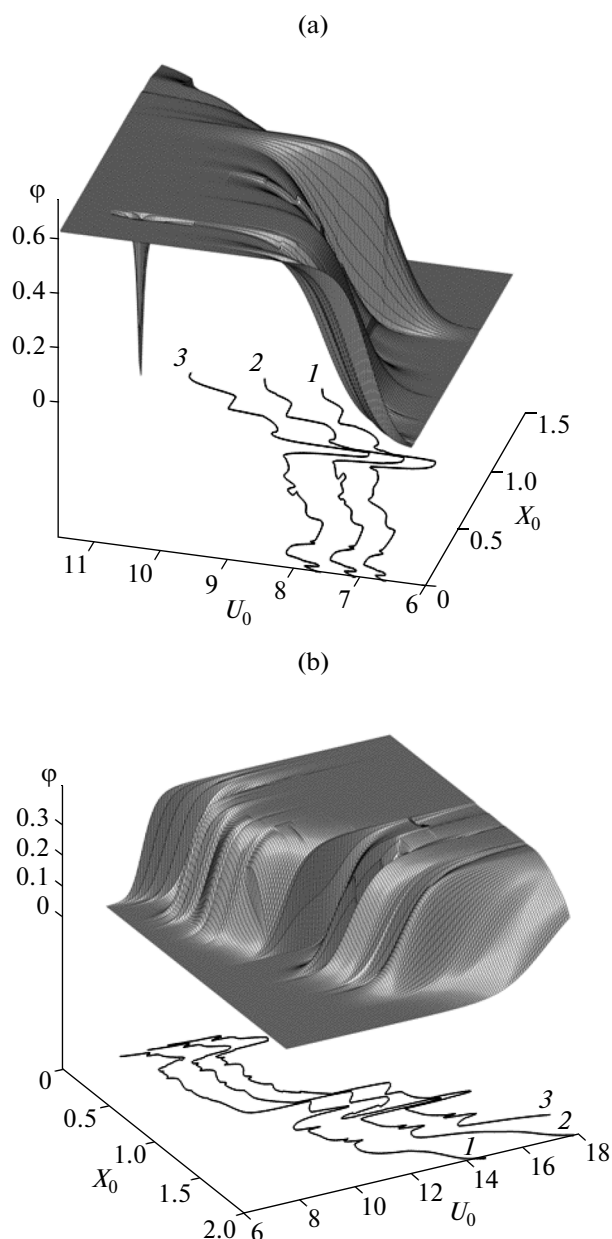


**Fig. 4.** Dependence of reaction quantum yield  $\phi$  upon the values of model parameters  $U_0$  and  $X_0$  for reactions (a) (1) ( $\phi = (1) 0.05$ , (2) 0.25, or (3) 0.55) and (b) (5) ( $\phi = (1) 0.005$ , (2) 0.20, or (3) 0.35).

lated quantum yields of reactions with the experimental yields is achieved. The problem is that the model is semiempirical and its practical implementation requires the model parameters to have the property of transferability in a series of reactions of identical type. It is in this case only that the model will be prognostic and can be used to predict the course of photochemical reactions and their quantum yields.

In studying the predictive character of the model and determining its parameters that are optimal from this point of view, it is necessary to set the required

accuracy of prediction (degree of deviation from experimental values  $\phi_{\text{exp}}$ ). At the current stage of development of the theory, we cannot expect very high accuracy (e.g., an error of less than 10–20%) and meeting the requirement to predict the order of magnitude is already a satisfactory result showing that the theoretical method used holds promise. Note that prediction of a quantum yield at the level of its order of magnitude is quite sufficient for many photochemistry problems. We will proceed in the future from a prediction uncertainty of 50%, which is not only an acceptable, but also very good value in the theoretical simulation of photochemical reactions of complex molecules and prediction of quantum yields of such processes.

Figure 5 shows the bands of values for model parameters  $U_0$ ,  $X_0$  corresponding to theoretical values of the quantum yields that deviate from the experimental yields by no more than 50% ( $\phi_{\text{calc}} = \phi_{\text{exp}}(1 \pm 0.5)$ ) for reactions (1)–(5), (7), and (8). The boundaries of the bands correspond to functions  $U_0(\phi_{\text{calc}} = 1.5\phi_{\text{exp}}) = f(X_0)$  and  $U_0(\phi_{\text{calc}} = 0.5\phi_{\text{exp}}) = f'(X_0)$ . For reactions (9) and (10), only the lower bounds of the bands are shown, since the maximum theoretical value for these reactions is  $\phi_{\text{max}} = 0.5\phi_{\text{exp}}$  as noted above. According to published experimental data [3], reactions (4) and (5) do not proceed; i.e.,  $\phi_{\text{exp}} = 0$ . Therefore, Fig. 5a presents only the upper bound of the range of the parameters for which the theoretical value of the quantum yield was taken to be  $10^{-5}$ . All the sets of parameters ( $U_0$ ,  $X_0$ ) lying below this line give a value of  $\phi_{\text{calc}} < 10^{-5}$  for reactions (4) and (5).

Experimental data for reaction (6) are controversial ( $\phi_{\text{exp}} = 0.3$  or  $0.03$  [3]), so the relevant bands of parameters are not given in Fig. 5a to avoid its overloading.

Figure 5 shows that, first, all the reactions are clearly grouped according to their type and the bands corresponding to different types of reactions are greatly separated in the space of parameters  $U_0$  and  $X_0$ . For example, the ranges of values of  $U_0$  are approximately as follows:  $6.2 < U_0 < 6.5$  for reactions (7) and (8),  $7.1 < U_0 < 7.8$  for reactions (1)–(5), and  $9.0 < U_0$  for reactions (9) and (10). This result is very important because, on one hand, there is no reason to expect the closeness of the model parameters for the reactions of different types even with slightly different values of their quantum yields and, on the other hand, this group of reactions is sufficiently representative by types. This shows the correctness of the theoretical model and makes it possible to predict the type of the chemical reaction of interest and its physicochemical properties in a complicated case. Second, the bands of values of model parameters for reactions of the same type overlap and there is an area (shaded in Fig. 5) common to all reactions of this type.

Thus, we arrive at the important conclusion that it is possible to find optimal parameters ensuring the

desired accuracy of the prediction for all reactions of the same type, that is, the property of transferability of parameters in a series of similar reactions is confirmed.

The ranges of optimum values of  $U_0$ ,  $X_0$  are wide enough and any point in these ranges (its corresponding model) gives the theoretical result required by the prediction level (50% in this case). To select the most preferred model, we will base on the following criteria. The principal criterion is that the number of normal coordinates for which the procedure of accounting the potential surface asymmetry should be minimal. In accordance with this requirement, let us impose a deliberately low limit of  $N_Q \leq 45\%$  for reactions (1)–(7) and  $N_Q \leq 50\%$  for reactions (9) and (10) (see above). The second criterion follows from the requirement of simplicity (uniqueness) of the choice of resonant levels in the calculation of the quantum yields of the reactions and consists in imposing the restriction  $\xi \leq 0.4$  (see above). Figure 5 shows the lines that correspond to these conditions and limit the range of possible values of model parameters  $U_0$  and  $X_0$ . A more stringent condition of  $\xi \leq 0.2$  is imposed on reactions (1)–(5) (Fig. 5a), since they are characterized by a very small value of  $\xi$  over a wide range of  $U_0$  and  $X_0$  values, as shown by calculations.

Thus, acceptance regions (indicated by double hatching in Fig. 5) for model parameters  $U_0$  and  $X_0$  corresponding to the initial requirements imposed on both the prediction accuracy and the physically substantiated model properties characterized by values of  $N_Q$  and  $\xi$  are distinguished for each of the above types of reactions. On one hand, these regions are relatively small so that they substantially differ in their location in the parameter plane for different reaction types, which is important, for example, for attributing a reaction to a particular type. On the other hand, they are large enough for a high degree of confidence that the optimal values of model parameters will lie in these ranges and the formulated physical requirements will be fulfilled for a significantly larger number of reactions of each type than the number considered here.

Under the constraints imposed, we select the optimum values of  $U_{\text{opt}}$  and  $X_{\text{opt}}$  that ensure the best agreement with the experimental quantum yields in each group reactions. Graphically, this corresponds to points  $(U_{\text{opt}}, X_{\text{opt}})$  that have the smallest total deviation from the  $U_0(\varphi_{\text{calc}} = \varphi_{\text{exp}}) = f(X_0)$  curves for groups of reactions. These points are marked in Fig. 5.

The obtained optimal values of the parameters and calculated quantum yields are given in Table 1. It is clearly seen that there is a very high prediction accuracy, which meets the preset initial requirements ( $\delta\varphi \leq 50\%$ ) for all of the reactions. The prediction uncertainty is less than 10% in most cases, (reactions (2), (4), (5), (7), (8), and (10)) and 20% in two cases (reactions (1) and (3)). Even for reaction (6) despite conflicting experimental data ( $\varphi_{\text{exp}} = 0.3$  or 0.03 [3]), the

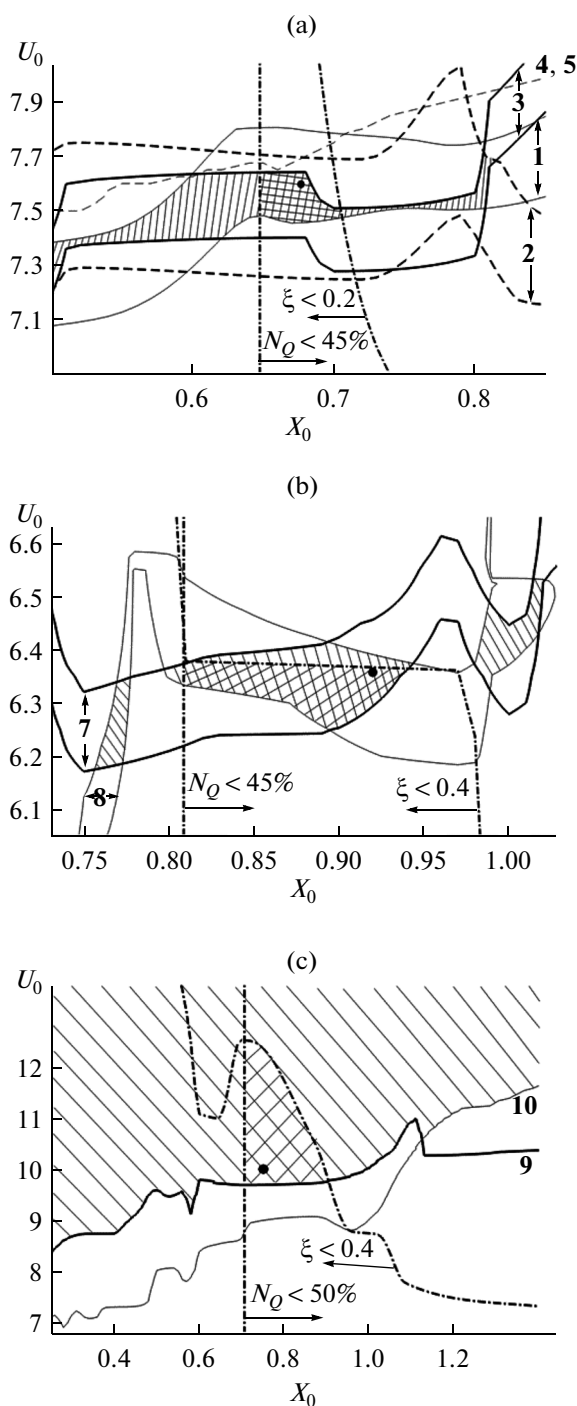


**Fig. 5.** Bands of values of model parameters  $U_0$  and  $X_0$  corresponding to theoretical quantum yield values that deviate from the experimental yields by no more than 50% for reactions (a) (1)–(5), (b) (7) and (8), and (c) (9) and (10). The boundaries of the ranges of the parameter in which  $N_Q$  is (a, b)  $< 45\%$  and  $\xi$  is (b, c)  $< 0.4$  or (a)  $< 0.2$  are shown, as well as points  $(U_{\text{opt}}, X_{\text{opt}})$  (●) corresponding to the optimal values of  $U_0$  and  $X_0$ . The shaded areas are those of the overlap of the bands of reactions of the same type, and double hatching highlights the areas that meet the boundary conditions in terms of  $N_Q$  and  $\xi$ .

Optimal values for model parameters ( $U_{\text{opt}}$ ,  $X_{\text{opt}}$ ) of molecules, calculated ( $\varphi_{\text{calc}}$ ) and experimental ( $\varphi_{\text{exp}}$ ) values of the quantum yield of reactions, deviations of the calculated form the experimental values ( $\delta\varphi = |\varphi_{\text{calc}} - \varphi_{\text{exp}}|/\varphi_{\text{exp}} \times 100\%$ ), the proportion of the normal coordinates ( $N_Q$ , %) for which the transformation by the potential energy surface is performed with allowance for its asymmetry, and values of parameter  $\xi$

| Reaction group | $U_{\text{opt}}$ | $X_{\text{opt}}$ | Reaction  | $\varphi_{\text{calc}}$ | $\varphi_{\text{exp}}$ [3] | $\delta\varphi$ , % | $N_Q$ | $\xi$ |
|----------------|------------------|------------------|-----------|-------------------------|----------------------------|---------------------|-------|-------|
| I              | 7.59             | 0.68             | <b>1</b>  | 0.072                   | 0.09                       | 20                  | 42    | 0.2   |
|                |                  |                  | <b>2</b>  | 0.130                   | 0.12                       | 8                   | 35    | 0.2   |
|                |                  |                  | <b>3</b>  | 0.036                   | 0.03                       | 20                  | 38    | 0.2   |
|                |                  |                  | <b>4</b>  | $10^{-15}$              | 0                          | —                   | 33    | 0.2   |
|                |                  |                  | <b>5</b>  | $10^{-6}$               | 0                          | —                   | 44    | 0.2   |
|                |                  |                  | <b>6</b>  | 0.6                     | 0.3, 0.03                  | 100                 | 35    | 0.1   |
| II             | 6.36             | 0.92             | <b>7</b>  | 0.032                   | 0.03                       | 6                   | 32    | 0.3   |
|                |                  |                  | <b>8</b>  | 0.012                   | 0.013                      | 6                   | 40    | 0.4   |
| III            | 10.0             | 0.75             | <b>9</b>  | 0.18                    | 0.35                       | 49                  | 50    | 0.3   |
|                |                  |                  | <b>10</b> | 0.28                    | 0.3                        | 8                   | 40    | 0.4   |

result obtained turns to be satisfactory as the theoretical value of  $\varphi_{\text{calc}} = 0.6$  correctly reproduces the order of magnitude of the quantum yield ( $\delta\varphi \leq 100\%$  for  $\varphi_{\text{exp}} = 0.3$ ).

Reaction (**9**) stands out by a relatively high uncertainty close to 50% in comparison with the other reactions. Although this result is satisfactory and consistent with the preset initial conditions, it is worth to note that the calculated values for the quantum yields of reactions (**9**) and (**10**) of group III are close to the maximum theoretical values ( $\varphi_{\text{calc}} \approx \varphi_{\text{max}}$ ) in the model approach. Apparently, the possibility that the multi-level resonance of vibronic states plays an essential role for these reactions was not taken into account in this calculation. This ignorance is indicated by the very “dense” pattern of the histograms of distribution of the normal coordinates over the deviations of the potential well minima from the top of the barrier, so that it is hard (impossible) to distinguish a small number of vibrations playing a key role in the structural transformation process. It is also manifested in the high values of  $N_Q$  in this calculation ( $N_Q = 50\%$  for reaction (**9**)). As has been shown in [27], the multilevel nature of the resonance leads to an increases in the quantum yields of the reactions. This feature is impor-

tant, and it can be taken into account in the given method of simulation of photochemical reactions [27].

## CONCLUSIONS

The results of the study show the possibility of predictive calculations of the kinetics and quantum yields of photochemical transformations of polyatomic molecules with satisfactory accuracy of the prediction and effectiveness of the quantum-chemical approach, developed for this purpose, using the optimized molecular model.

With allowance for the physically sound requirements and rather stringent constraints imposed on the prediction error (less than 50%), a satisfactory theoretical result has been achieved for all of the reactions attributed to the three chemically different types. In most cases (eight out of ten reactions), the deviation from the experimental data is less than 20%.

The model used has the property that a common range of possible values of the model parameters ensuring the required level of quantitative prediction is allocated for reactions belonging to the same chemical type. This property demonstrates the transferability of

the parameters of the model in a series of reactions of the same type.

Such areas for different types of reactions are strongly separated in the space of model parameters. This apartness not only shows the correctness of the theoretical model used, but also makes it possible to theoretically predict in complex cases the type of the reaction in question and its physicochemical characteristics.

## REFERENCES

1. Terenin, A.N., *Fotonika molekul krasitelei i rodstvennykh organicheskikh soedinenii* (Photonics of Dyes and Related Organic Compounds), Leningrad: Nauka, 1967.
2. Turro, N.J., *Molecular Photochemistry*, New York: Benjamin, 1965.
3. Calvert, J.G. and Pitts, J.N., *Photochemistry*, New York: Wiley, 1966.
4. Bagdasar'yan, Kh.S., *Dvukhkvantovaya fotokhimiya* (Two-Quantum Photochemistry), Moscow: Nauka, 1976.
5. Chibisov, A.K. *Usp. Khim.*, 1981, vol. 50, no. 7, p. 1169.
6. Molin, Yu.N., Panfilov, Yu.N., and Petrov, A.K., *Infrakrasnaya fotokhimiya* (Infrared Photochemistry), Novosibirsk: Nauka, 1985.
7. Wayne, R.P., *Principles and Applications of Photochemistry*, Oxford: Oxford Univ. Press, 1988, 2nd ed.
8. Michl, J. and Bonacic-Koutecky, V., *Electronic Aspects of Organic Photochemistry*, New York: Wiley, 1991.
9. Klessinger, M. and Michl, J., *Excited States and Photochemistry of Organic Molecules*, New York: Wiley-VCH, 1995.
10. *Surface Photochemistry*, Anpo, M., Ed., New York: Wiley, 1996.
11. Maier, G.V., Artyukhov, V.Ya., Bazyl', O.K., Kopylova, T.N., Kuznetsova, R.T., Rib, N.R., and Sokolova, I.V., *Elektronno-vozbuzhdenные sostoyaniya i fotokhimiya organicheskikh soedinenii* (Electronically Excited States and Photochemistry of Organic Compounds), Novosibirsk: Nauka, 1997.
12. Coyle, J.D., *Introduction to Organic Photochemistry*, New York: Wiley, 1998.
13. *Advances in Photochemistry*, vol. 29, Neckers, D.C., Jenks, W.S., and Wolff, T., Eds., Hoboken, N.J.: Wiley, 2007.
14. Turro, N.J., Ramamurthy, V., and Scaiano, J.C., *Principles of Molecular Photochemistry: An Introduction*, Mill Valley, CA: University Science Books, 2009.
15. Wardle, B., *Principles and Applications of Photochemistry*, New York: Wiley, 2009.
16. Klan, P. and Wirz, J., *Photochemistry of Organic Compounds: From Concepts to Practice*, Chichester: Wiley, 2009.
17. *Supramolecular Photochemistry: Controlling Photochemical Processes*, Ramamurthy, V. and Inoue, Y., Eds., Hoboken, N.J.: Wiley, 2011.
18. Gribov, L.A. and Baranov, V.I., *Teoriya i metody rascheta molekulyarnykh protsessov: spektry, khimicheskie prevrashcheniya i molekulyarnaya logika* (Theory and Methods of Calculation of Molecular Processes: Spectra, Chemical Transformations, and Molecular Logics), Moscow: KomKniga, 2006.
19. Gribov, L.A. and Baranov, V.I., *High Energy Chem.*, 2010, vol. 44, no. 6, p. 462.
20. Baranov, V.I., Gribov, L.A., Dridger, V.E., Iskhakov, M.Kh., and Mikhailov, I.V., *High Energy Chem.*, 2009, vol. 43, no. 5, p. 362.
21. Baranov, V.I., Gribov, L.A., Dridger, V.E., Iskhakov, M.Kh., and Mikhailov, I.V., *High Energy Chem.*, 2009, vol. 43, no. 6, p. 489.
22. Baranov, V.I., Gribov, L.A., Dridger, V.E., and Mikhailov, I.V., *High Energy Chem.*, 2010, vol. 44, no. 3, p. 181.
23. Baranov, V.I., Gribov, L.A., Iskhakov, M.Kh., and Mikhailov, I.V., *High Energy Chem.*, 2010, vol. 44, no. 4, p. 277.
24. Baranov, V.I., Gribov, L.A., Iskhakov, M.Kh., and Mikhailov, I.V., *High Energy Chem.*, 2011, vol. 45, no. 6, p. 486.
25. Baranov, V.I., Gribov, L.A., and Pavlyuchko, A.I., *Khim. Vys. Energ.*, 2013, vol. 47, no. 1, p. 52.
26. Baranov, V.I., Gribov, L.A., Mikhailov, I.V., and Poteshnaya, N.I., *High Energy Chem.*, 2014, vol. 48, no. 1, p. 30.
27. Gribov, L.A. and Baranov, V.I., *High Energy Chem.*, 2010, vol. 44, no. 6, p. 462.

Translated by S. Zatonsky